University of Wisconsin Milwaukee

UWM Digital Commons

December 2020

The Instability of Verge-Foliot Clocks in Contrast with the Isochronicity of Pendulum Clocks: A Study of Verge-Foliot Kinematics

Aaron Seth Blumenthal
University of Wisconsin-Milwaukee

Follow this and additional works at: https://dc.uwm.edu/etd

 Part of the Mechanical Engineering Commons

THE INSTABILITY OF VERGE-FOLIOT CLOCKS IN CONTRAST WITH THE ISOCHRONICITY OF PENDULUM

CLOCKS: A STUDY OF VERGE-FOLIOT KINEMATICS

by

Aaron Seth Blumenthal

A Thesis Submitted in

Partial Fulfillment of the

Requirements for the Degree of

Master of Science

in Engineering

at

The University of Wisconsin-Milwaukee

December 2020

ABSTRACT

THE INSTABILITY OF VERGE-FOLIOT CLOCKS IN CONTRAST WITH THE ISOCHRONICITY OF PENDULUM
CLOCKS: A STUDY OF VERGE-FOLIOT KINEMATICS

by

Aaron Seth Blumenthal

The University of Wisconsin-Milwaukee, 2020
Under the Supervision of Professor Michael Nosonovsky

The tower clocks of Europe starting in the 13th century CE employed a verge-foliot mechanism, which was low in both precision and accuracy due to the sensitivity of frictional losses in the system. The pendulum and Huygens' introduction of the Theory of Involutes is shown to be a mechanism with a linear relationship to frictional losses in the system, instead of the non-linear relationship between frictional losses in verge-foliot mechanisms. The isochrone nature of vibrations of the pendulum are discussed in contrast to the variance in oscillation seen in verge-foliots. The introduction of the pendulum resulted in an improvement of accuracy of around $\pi/\mu \approx 31$ times, where $\mu=0.1$ is the coefficient of friction. In this thesis a CAD model is developed for both the verge-foliot and pendulum with a verge, and it is found that FEA analysis produces a sufficiently approximate result to the theoretical models. A discussion of CAD and DFM principles in relation to clocks is also discussed.

To

my wife,

my family,

my friends,

and my best friend Zorro

TABLE OF CONTENTS

LIST OF FIGURES

LIST OF ABBREVIATIONS

CAD	Computer-Aided Design
CAM	Computer-Aided Manufacturing
FEA	Finite Element Analysis
FEM	Finite Element Method
CAE	Computer-Aided Engineering
SLDPRT	SolidWorks Part File Format
STEP	Standard for the Exchange of Product Model Data File Format
ASME	American Society of Mechanical Engineers
ANSI	American National Standards Institute
DIN	Deutsches Institut für Normung (German Institute for Standardization)
ISO	International Organization for Standardization
NIST	National Institute of Standards and Technology
BOM	Bill of Materials
ODE	Ordinary Differential Equations
PDE	Partial Differential Equations
CE	Common Era
SAE	Society of Automotive Engineers
AISI	American Iron and Steel Institute
UNS	Unified Numbering System
ASTM	American Society for Testing and Materials
FDM	Fused Deposition Modeling
FFF	Fused Filament Fabrication
PLA	Polylactic Acid $(C_3H_4O_2)_n$

ACKNOWLEDGMENTS

First and foremost, I want to thank my advisor, Dr. Michael Nosonovsky, for helping guide me through the process of writing a thesis and for sending our work to numerous publications to get published. I wish to thank Helen Chapman, Secretary of the Antiquarian Horological Society for helping me access materials of the society. I would also like to thank Dr. Nathaniel Stern and Dr. Ilya Avdeev for serving on my thesis defense committee.

1. Objective

The objective of this thesis to develop a mathematical model to investigate the reason verge-foliot mechanisms are substantially less accurate than pendulums with a verge mechanism, investigate the effect of friction on the stability of both the verge-foliot and the pendulum mechanisms, and to gain insights on the improved performance of the pendulum using computer simulations of the verge-foliot mechanism based on a typical historical example of a chamber clock.

2. Introduction

From time immemorial, time accounting and measurement has had profound impacts on society and the sciences. For early humans, time was measured by organic means, whether it was the setting of the Sun, the arrival of a full Moon, or the changing of the seasons. Our sense of time as constant unit began to shift with the development of larger agrarian societies that allowed for the existence of a learned class. The Egyptians were the first recorded society that divided the day up into smaller parts, however, it was not until the Hellenistic Age that the concept of the hours being fixed in length was conceived by the astronomer Hipparchus. Hipparchus proposed dividing the day into 24-hour segments, with those hours being divided further into 60 minutes (Robertson & O'Connor, Hipparchus of Rhodes, 1999). The system Hipparchus proposed for both timekeeping and longitudinal coordinates was based off the sexagesimal system developed millennia earlier by the Sumerians, among the first agrarian, organized civilizations (Lombardi, 2007). These early civilizations used various methods of time, with clepsydrae and sundials being the most common, both of which can be found in early civilizations around the globe. Clepsydrae have been found in ancient China, India, Egypt, Persia, Korea, and Babylon (Britten, Clutton, Baille, Baillie, & Ilbert, 1973). Yi Xing of the Tang Dynasty has been credited as inventing the first clockwork escapement, however, this was on a clepsydra, and was more of a flow regulator than an escapement in the modern sense of the word (Cipolla, 2003). Such flow regulation inspired the medieval Muslim engineer Ismail al-

Jazari in Anatolia, who developed a complex water clock using gearing, water wheels, and weight driven mechanisms in the 12th century CE. The most famous of these clocks is his "Elephant Clock" as seen in Figure 1 (al-Razzaz al-Jazari & `Abd al-Latif, 1315).

Figure 1 The Elephant Clock made by Ismail al-Jazari was a clepsydra that utilized a primitive escapement, Metropolitan Museum of Art (al-Razzaz al-Jazari & `Abd al-Latif, 1315) (Creative Commons CC0 1.0)

A flurry of activity began in the early Medieval Period in Europe with the development of both the hourglass and the mechanical clock. The mechanical clock was invented in the 13th century CE, right around the same time that the hourglass reached the peak of its popularity (Cipolla, 2003). As time discipline became a more necessary practice, the mechanical clock was able to decrease in cost and increase in accuracy. This increase in accuracy and availability of mechanical timekeeping devices that proved to be one of the most important periods in history: time becomes fungible, and as the philosopher Lewis Mumford states in his pivotal work Technics and Civilization, "as [time keeping becoming more

accurate] took place, Eternity ceased gradually to serve as the measure and focus of human actions…the clock, not the steam-engine, is the key machine of the modern industrial age" (Mumford, 2010). Now, the weather and climate no longer needed to impact timekeeping, where clepsydrae would freeze on cold nights and sundials would not be able to work at night or with cloud cover, the mechanical clock was able to continue keeping time.

The earliest of these mechanical clock makers were primarily monks, as a strict time regimen was important to religious orders who wanted to provide a sense of regularity and order to contrast the violent dislocation of society in the wake of the fall of the Roman Empire (Evans, 2007). These early clocks would hardly be called clocks by most modern definitions, as there was no face and its only external output was the ringing of bells or chimes at regular intervals, but many mechanical solutions had been derived to get even these seemingly simple machines to function. Regular, periodic, or oscillatory motion was used to achieve accurate time measurement. An escapement mechanism regulated the motion of the clock by periodically limiting the motive force; without such limiting the motive force would quickly exhaust itself. The first such escapement that was developed was the verge-foliot escapement; it was this escapement that would help John Harrison solve the problem of longitude for navigation at sea centuries later (Moon & Stiefel, 2006). As opposed to John Harrison's metallurgically advanced and temperature compensating mechanism, early verge-foliot clocks were inaccurate affairs by being off by around one to two hours a day (Cipolla, 2003). The losses in the system can occur due to the fundamental nature of how the escapement works, as seen in Figure 2. A motive force, most often a weight driven pulley, spins the crown wheel which in turn elastically collides with two pallets that are attached to a shaft with a high moment of inertia due to the attachment of weights. These weights are arranged in a way where their distance to the axis of rotation on the foliot can be adjusted, thus adjusting the moment of inertia of the mechanism. This allows the governor of the clock to change the going rate and adjust the clock hours to match the changing lengths of days throughout the year (Britten, Clutton, Baille, Baillie, & Ilbert, 1973).

3

The verge mechanism has been studied as an early feedback mechanism. Lepschy used a comparison of the Ktesibios' water clock with the verge mechanism to show examples of feedback loops (Lepschy, Mian, & Viaro, 1992). Several other papers and textbooks have studied, but not to answer for what reasons the accuracy of verge-foliot clocks were roughly 30 times as inaccurate as pendulum clocks.
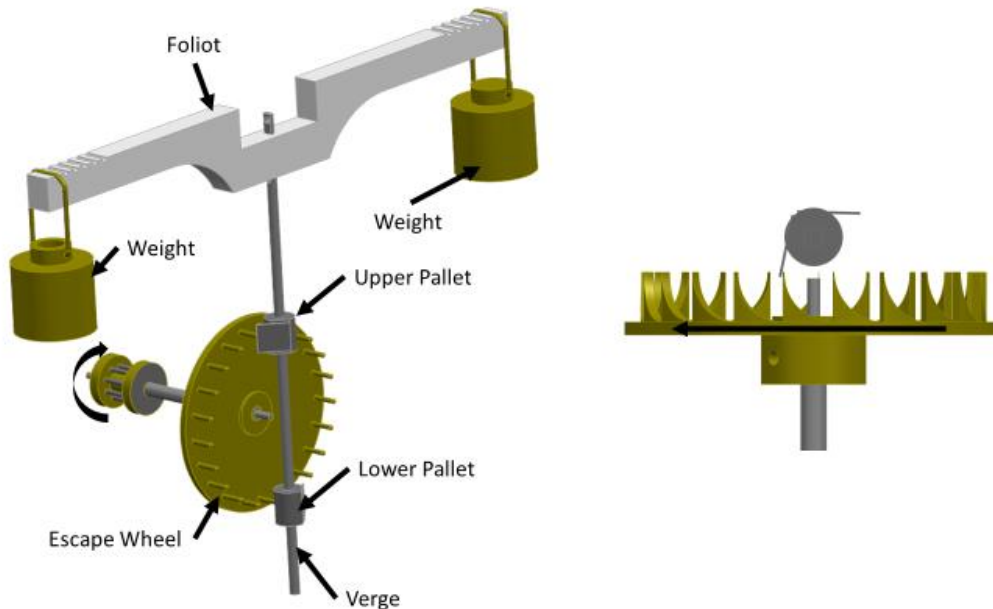
Figure 2 Schematic of Verge-Foliot

3. The Medieval and Early Modern Tower Clocks

In this chapter, pre-pendulum tower clocks and the impact of the invention of the pendulum are reviewed. The development of oscillatory feedback systems during the thirteenth and fourteenth centuries was an important development in mechanism design. An overview of several example tower clocks and the changes that the pendulum brought about are discussed.

3.1 Pre-Pendulum Tower Clocks

Clocks began to change from clepsydra towards more mechanical means sometime in the second half of the 13th century. Villard de Honnecourt, a 13th century architect from northern France, produced a portfolio showing numerous mechanical devices, images of people and animals, and other assorted material both religious and secular; in this work, dated to have been drawn between 1225 CE and 1251, shows, in Figure 3, a figure that appears to be an early example of a mechanical escapement (Price, 1959). It however is not until the 1362 CE construction of the *Tour de l'Horloge* tower clock in Paris by Henri de Vick, of which there are numerous drawings of its going train, that it can be concretely showed that the verge-foliot was used (Brearley, 1919).
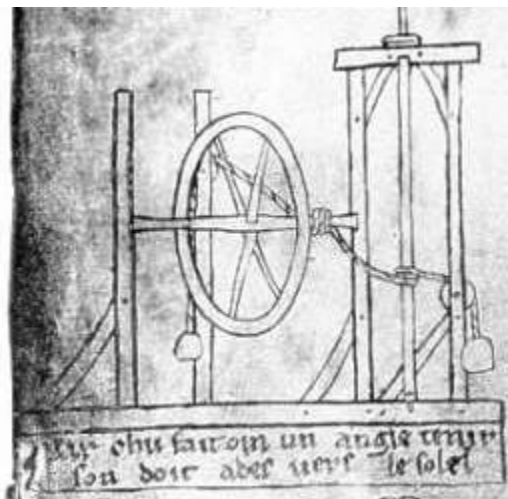
Figure 3 Villard de Honnecourt Foliot 44 illustrating a supposed escapement (Honnecourt, 1230) (Public Domain)

The *Astrarium* astronomical clock was finished 2 years later in 1364 by Giovanni Dondi dell'Orologio is also known to have used a verge escapement but used a crown or balance wheel instead of a foliot (Blumenthal & Nosonovsky, 2020), as seen in Figure 4. The *Astrarium* is also illustrated in the accompanying manuscript *Tractatus Astrarii* also by Giovanni Dondi (Cipolla, 2003). There is a possibility that the first clock was finished in 1283 at the Priory Church in Dunstable, England, however, this cannot be confirmed (Evans, 2007). There is also speculation that first mechanical tower clock could have been

at the San Gottardo church in Milan in the year 1335, due to its description of having a striking and a driving train (Kleinschmidt, 2000). There was a flurry of tower clocks constructed around Italy in the 1340s and 1350s. The next wave of clock tower construction in the second half of the 14th century swept through France, Germany, and England. The clock in Strasbourg, France, erected in 1352, is widely viewed as the first clock tower outside of Italy (Britten, Clutton, Baille, Baillie, & Ilbert, 1973).
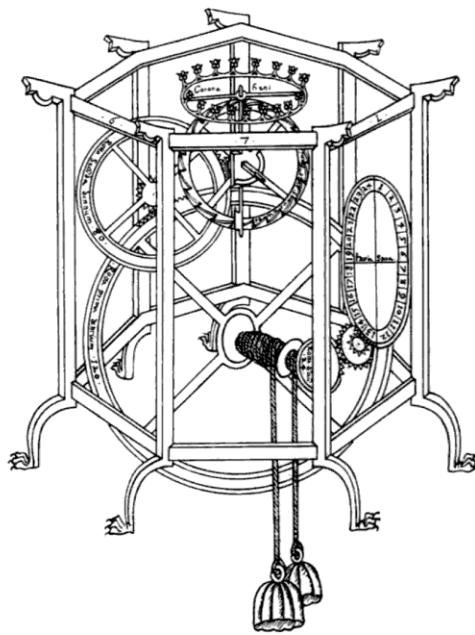
Figure 4 Astrarium astronomical clock was finished 2 years later in 1364 by Giovanni Dondi dell'Orologio, note the use of a balance wheel instead of a foliot (de Dondi, 1461) (Public Domain)

The construction of these early tower clocks is generally similar. The clocks are made from wrought iron, with a few exceptions being made of wood. The movement is housed in an open frame, referred to as a "birdcage" for its open appearance, as seen in Figure 5. Tenons, mortises and wedges are used to keep the parts in place, and the drive train is usually end-to-end, as opposed to the side-by-side birdcage style common after the invention of the pendulum (McKay, 2016). The verge-foliot along with the crown wheel were most often positioned in the middle of the frame and supported by beams. Bushings were

also made of wrought iron, although this began to change to brass in the second half of the 15th century

(Frank, The Evolution of Tower Clock Movements and Their Design Over the Past 1000 Yearks, 2013).
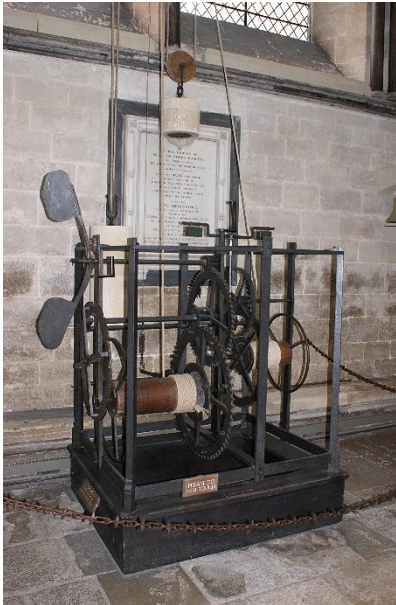
Figure 5 Salisbury Cathedral Clock
(Llewelyn, 2014) (Creative Commons 3.0)

Doorframe and field gate frames and housings were also used to support the going trains of some early

tower clocks, however, there are few extant examples. The doorframe housing is most notable in that the

verge-foliot escapement is in an inverted position; the most notable example of this can be seen in the

Cotehele Clock (Fig. 6) (Frank, The Evolution of Tower Clock Movements and Their Design Over the Past

1000 Yearks, 2013), erected between 1493 and 1521, and still in use today. The winding system to provide

the motive force necessary to drive the clock were often provided by a weight on the end of a rope

wrapped around a capstan, like those found in the rigging of sailing vessels. The weight would then have

to be reset to its initial position periodically by the clock governor through various means ranging from

fixing the rigging of the capstan by hand to various methods of human power mechanical winches and

windings. Remontoir mechanisms, which rewinds and resets the motive power for a clock were invented

by Swiss clockmaker Jost Burgi in around 1595 by using gravity (Robertson & O'Connor, Jost Bürgi, 2010).

Jost Burgi later refined the concept of the remontoir into the spring remontoir in 1615 (Frank, Wagner Remontoir, 2008). These mechanisms, in particular the spring remontoir applied to ensuring the verge pallets have constant contact with the crown wheel, improved the accuracy of the verge-foliot; they also were the precursors to the mechanisms necessary to produce accurate watches. Despite these vast improvements in the accuracy of the verge-foliot mechanism, the noncontiguous improvement in accuracy of the pendulum thoroughly supplanted verge-foliot use in publicly funded clocks (Cipolla, 2003) (Brearley, 1919).

Figure 6 Cotehele Clock with its inverted foliot (Denning, 2007)
(Creative Commons 3.0)

3.2 Impact of the Invention of the Pendulum on Time Measurement

As time passed, the need for ever more accurate clocks was assuaged by the invention of the pendulum.

Apocryphally, the pendulum was first conceived by a bored Galileo while sitting in church, observing a

swinging lantern, keeping track of the time of each swing by using his heartbeat. He noticed that no matter how high the lantern swung; the period of the swing was approximately independent of this height (Glasgow, 1885) (Brearley, 1919). This property, isochronicity, is invaluable to timekeeping, because the period of the timekeeping device would be independent of the amplitude of successive swings of the pendulum. However, it was not until Christiaan Huygens contracted out his idea for a clock that an actual pendulum clock was built in 1658 (Blumenthal & Nosonovsky, 2020). The pendulum dropped the error per day down from hours to seconds, a 30-fold increase in accuracy. Huygens further expounded on the mechanics of the pendulum in his work the *Horologium Oscillatorium* in 1673. Huygens provides explanations using theories of curves and evolutes to prove the existence of tautochrone curve; the book also provides solutions to compound pendulums, centers of oscillation and develops the concepts of the moment of inertia and centrifugal force. The tautochrone curve (Fig 7), also known as the isochrone curve, is a cycloidal curve along which pendulums will all have the same period. It was not until Joseph Lagrange and Leonhard Euler looked at the tautochrone curve that an analytical solution was provided (Speiser, 2008). Looking directly at the isochrone nature of a simple pendulum, the period of oscillation of a simple pendulum with a swing where the angle θ is sufficiently small enough that it can be used to approximate sin θ, is given by:

$$T = 2\pi \sqrt{\frac{L}{g}}$$

Where L is the length of the pendulum arm. The removal of energy losses in the inelastic collisions and friction of the verge-foliot mechanism, and the dependence only on the length of the pendulum arm greatly improved the accuracy of clocks.
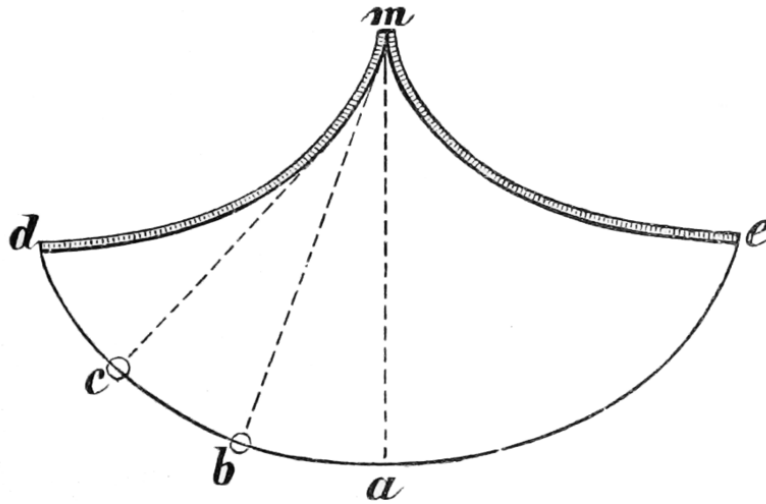
Figure 7 Tautochrone curve (Bisgaard, 2006) (Public Domain)

The Scientific Revolution of the 17th century CE coincided with the increase in accuracy of clocks. As Huygens, Newton, Galileo created methodical and repeatable concepts of how the world works, new scientific instruments were needed to prove these theories and others. Clocks and their makers were on the cutting edge of the development of such tools, ranging from metallurgy to the scientific theories themselves, clocks played a large and important part in these developments (Cipolla, 2003).

The increase in accuracy of clocks has also been postulated to be the precursor to the Industrial Revolution. One of the initial drivers of the Industrial Revolution was an increase in trading activity, resulting in the creation of businesses. This trade was aided by the invention of accurate clocks for use by boats to determine their longitude with great accuracy, increasing the speed and decreasing insurance costs on trading vessels. With greater trading came a need for more products by an increasingly urban workforce. It was the fungibility of time due to accurate clocks that allowed for more regimented commerce and means of employment. It is no wonder that the clock was one of the earliest mass-produced products, with the advent of truly interchangeable parts for clocks by the American inventor Eli Terry Jr., who was producing 3000 clocks per year, while skilled craftsmen at the time could only produce six to ten clocks per year (Vaughn, 2019). At the same time, there was a move towards a global

11

standardization of time; railroads running between cities and countries required a standardized time to ensure that accurate timetables could be produced (Mumford, 2010). Time was wholly inorganic at this point, completely distinct from the wills of Nature.

The pendulum was considered the most accurate timekeeper until the invention of the quartz clock in 1927, which uses electronic oscillation instead of mechanical oscillation (Marrison, 1948). The oscillation of the quartz crystal produces a signal with precise frequency. The first widely available commercial use of the quartz clock, in 1969 with the Seiko Astron (IEEE Tokyo Section, 2004), but it was not until the 1980s that quartz clocks had become ubiquitous.

4. Dynamic Modeling of The Verge-And-Foliot Mechanism

In this section, the modeling of the verge-and-foliot and the verge-pendulum mechanisms are discussed. The importance of friction in the accuracy discrepancy between the two mechanisms is explained, followed by a comparison of the stability analyses of both mechanisms.

4.1 Mechanics of the Verge-and-Foliot Mechanism

The verge escapement has two component sets: a set that drives the mechanism and a second set that regulates the period of oscillation. The driving aspect of the verge escapement mechanism consists of a weight driven crown wheel, sometimes referred to as a contrate gear, of an odd number of evenly spaced asymmetrical saw teeth (Glasgow, 1885). The driving weight is assumed to provide a constant torque on the crown wheel. The crown wheel periodically collides with the opposingly positioned pallets that are fastened to the verge. The axis of rotation of the verge is perpendicular to the axis of rotation of the crown wheel. The pallets positioned along the shaft separated by roughly the diameter of the crown wheel, and with an angular separation ranging from 90° to 115° but is most often taken to be approximately 100°. The verge is fixed to either a foliot or a pendulum and allowed to freely rotate. The foliot is a perpendicular beam attached to one end of the verge. The foliot has moveable weights on it positioned equidistantly

from the axis of rotation to adjust its moment of inertia. The rotational movement of the crown causes an alternating rotational movement of the verge-foliot; the movement of the crown wheel pushing on the upper pallet causes an anticlockwise rotation in the verge-foliot, whereas a push on the lower pallet results in an opposite, clockwise rotation. During the rotation of the verge-foliot, the pallets move approximately the angle of $\Delta\varphi \approx 100°$ before it releases the tooth to allow the other pallet to engage the crown wheel; the crown wheel during the drop (or free rotation) roughly 2°. This process of impact, free rotation, and impact continues indefinitely, or until the crown wheel motive force needs to be reset. The verge-foliot arrangement is positioned with the rotational axis of the verge being vertical with respect to the surface of the Earth; however, when the verge is fixed to a pendulum the axis of rotation of the verge is horizontal with respect to the surface of the Earth.

In additional to the foliot, a balance wheel was sometimes used in its place, most often seen in clocks that were not turret clocks. The balance wheel is a strip of metal or weighty material in the shape of a circle affixed to the verge. The balance wheel has the advantage of both temperature changes and aerodynamic dynamic drag having reduced impact on the oscillation of the mechanism. The movement and escapement were also greatly improved around the 1560's CE by using brass bushings on wrought iron instead of simple journal bearings of the same wrought iron material throughout (Frank, The Evolution of Tower Clock Movements and Their Design Over the Past 1000 Yearks, 2013). The dissimilar rubbing surfaces of the improved bearings reduced the amount of wear, which increases the coefficient of friction over time.

The replacement of the foliot and the balance wheel with the pendulum by Huygens, the second version of his clock built in 1673 CE, resulted in an accuracy of 10 seconds per day, which is a roughly 31 times increase from the accuracy of contemporary verge-foliot clocks (Blumenthal & Nosonovsky, 2020). This early pendulum still required a large angular movement, as seen in Figure 8, causing the movement of the pendulum mass to move in a manner outside the bounds of a tautochrone or isochrone curve; this is the reason for the improved accuracy of the pendulum clocks with the invention of the anchor

13

escapement, which reduced the angular arc from 100° to roughly 5° (Headrick, 2002). The near

harmonic oscillatory nature of pendulums with small displacement provides the basis of the modern

conception of time measurement and spurred subsequent inventions in the field of escapements.

Verge-and-Foliot   Verge and Pendulum
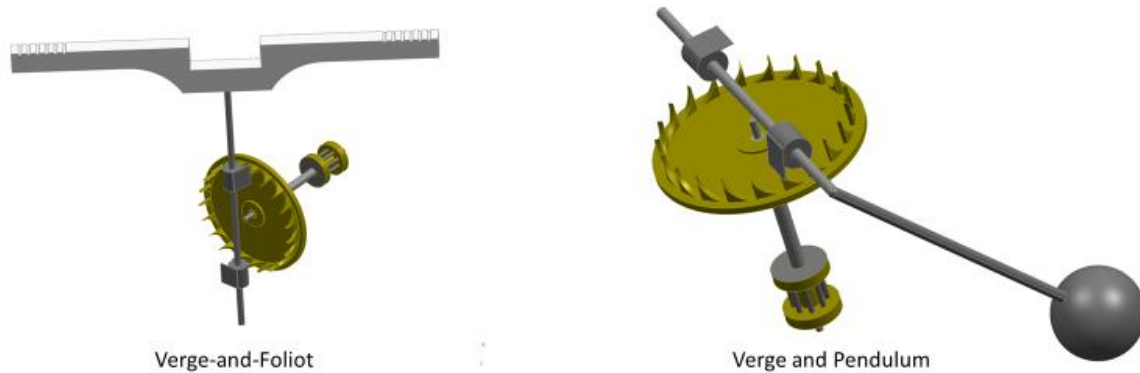
Figure 8 Comparison of the verge mechanism with a foliot and a pendulum. Note the difference in escapement wheel orientation

The operation of the driving component set is straightforward; it only drives in one direction (traditionally

clockwise). The crown wheel's angular velocity is changed by the verge-foliot; this operation can be

divided into six different periods:

1. The verge-foliot has a force acted upon them in a clockwise fashion via the driven crown wheel contacting the top paddle on the verge.

2. The geometry of the verge-foliot and the crown wheel make it so that they lose contact with each other and freely spin both in a clockwise direction (also known as the drop). The angular velocity of the verge-foliot remains constant. The crown wheel accelerates without contact with the verge's paddle.

3. The bottom verge paddle contacts the crown wheel, and because of the geometry, is traveling in a direction that opposes the motion of the crown wheel. This causes a rapid negative acceleration of both the verge and the crown wheel.

4. The verge-foliot has a force upon them in a counterclockwise fashion via the driven crown wheel impacting the top paddle on the verge.

5. The verge-foliot and the crown wheel experience a drop and freely spin, the crown wheel in a clockwise direction and the verge-foliot in a counterclockwise direction. The angular velocity of the verge-foliot remains constant. The crown wheel accelerates without contact with the verge's paddle.

6. The top verge paddle contacts the crown wheel. This causes a rapid negative acceleration of both the verge and the crown wheel, bringing both almost to a standstill.

To ensure that the crown wheel and the paddles of the verge will engage, the following condition must be met:

$$R_c \sin \frac{\pi}{n} = R_v \sin \Delta\varphi$$

Where n is an odd number equal to the number of teeth, and $\Delta\varphi$ is the angle between the paddles. The number of teeth on the crown wheel must be an odd number to allow the pallets of the verge to disengage and freely move to engage the next tooth.

4.2 Mathematical Model of the Verge Escapement Mechanism with Foliot

Using the previous framework for the operation of the verge escapement mechanism and the kinematic set-up in my previous paper with Dr. Nosonovsky (Blumenthal & Nosonovsky, 2020), the following mathematical model is produced:

1. The crown wheel and the verge rotate in the same direction with the angular acceleration of

$$\ddot{\theta} = T/(J_C + J_V) \qquad \text{for } \varphi_0 \leq \varphi \leq \varphi_1 \text{ and } \dot{\varphi} \geq 0 \tag{1}$$

$$\dot{\varphi} = \dot{\theta}$$

where T is the torque exerted on the verge by the weight, J_C and J_V are the moments of inertia of the crown wheel and the verge-foliot, θ and φ are the rotation angles of the crown wheel and the verge, respectively. The values of φ_0 and φ_1 correspond to the two pallets hitting the teeth, so that $\Delta\varphi = \varphi_1 - \varphi_0 \approx 100°$.

2. The drop of the verge and the acceleration of the crown wheel continues until it moves for the distance of $\Delta\theta$, usually taken to be $\approx 2°$, and contacts the verge pallet:

$$\ddot{\theta} = T/J_C \qquad \text{for } \varphi_1 < \varphi \text{ and } \dot{\varphi} \geq 0, \int \dot{\theta} dt < \Delta\theta \tag{2}$$

$$\ddot{\varphi} = 0$$

3. The tooth hits the second pallet, when either an elastic or inelastic collision can occur. Typically, it is assumed that the collision is inelastic. This implies that while the total angular momentum is conserved after the collision, the angular velocities are

$$\dot{\varphi}_{after} = -\dot{\theta}_{after} = -\frac{(\dot{\theta}J_C + \dot{\varphi}J_V)}{J_C + J_V} \tag{3}$$

Energy dissipation via either inelastic collision or friction is necessary for the verge escapement mechanism to function and must be included. Without the dissipation the crown wheel would continuously accelerate, and the verge would not provide the constant rate of motion needed for proper time keeping.

4. The opposite motion of the crown wheel and the verge

$$\ddot{\theta} = T/(J_C + J_V) \qquad \text{for } \varphi_0 \leq \varphi \leq \varphi_1 \text{ and } \dot{\varphi} < 0 \tag{4}$$

$$\dot{\varphi} = -\dot{\theta}$$

5. The drop of the verge in the opposite direction and acceleration of the crown wheel:

$$\ddot{\theta} = T/J_C \qquad\qquad \text{for } \varphi < \varphi_0 \text{ and } \dot{\varphi} \leq 0, \ \int \dot{\theta}dt < \Delta\theta \qquad\qquad (5)$$

$$\ddot{\varphi} = 0$$

6. The tooth hits the first pallet.

$$\dot{\varphi}_{after} = \dot{\theta}_{after} = \frac{(\dot{\theta}J_C + \dot{\varphi}J_V)}{J_C + J_V} \qquad\qquad (6)$$

The above model does not take friction into consideration; however, a constant Coulomb friction torque, f, opposing the rotation of the crown-wheel can be easily added to the system by modifying the total torque as $T_f = T - f\,\text{sgn}\dot{\theta}$.

The total period of oscillation is equal to the sum of the durations of all six phases:

$$\tau = \sum_{n=1}^{6} \tau_n \qquad\qquad (7)$$

where $\tau_1 = \tau_4 = \sqrt{2\Delta\varphi(J_C + J_V)/T}$, $\tau_2 = \tau_5 = \sqrt{2\Delta\theta J_C/T}$, while $t_3 = t_6$ are small yielding the period of oscillations

$$\tau = \frac{2\sqrt{2}}{\sqrt{T}}\left(\sqrt{\Delta\varphi(J_C + J_V)} + \sqrt{\Delta\theta J_C}\right) \approx \frac{4\sqrt{2\Delta\varphi(J_C + J_V)}}{\sqrt{T}} = 4\sqrt{\frac{2(J_V + J_C)\Delta\varphi}{T}} \qquad\qquad (8)$$

4.3 Mathematical Model of the Verge Escapement Mechanism with Foliot

The model can be applied to the motion of the verge with the pendulum attached with the restoring torque of $k\varphi$. The six phases are then given by:

1. The crown wheel and the verge rotate in the same direction

$$\ddot{\theta} = (T - k\varphi)/(J_C + J_V) \qquad \text{for } \varphi_0 \leq \varphi \leq \varphi_1 \text{ and } \dot{\varphi} \geq 0 \qquad\qquad (9)$$

$$\dot{\varphi} = \dot{\theta}$$

2. The free motion of the verge

$$\ddot{\theta} = T/J_C \qquad\qquad (10)$$

$$\ddot{\varphi} = -k\varphi/J_V$$

3. The tooth hits the second pallet.

$$\dot{\varphi}_{after} = -\dot{\theta}_{after} = -\frac{(\dot{\theta}J_C + \dot{\varphi}J_V)}{J_C + J_V} \qquad\qquad (11)$$

4. The opposite motion of the crown wheel and the verge

$$\ddot{\theta} = \frac{T + k\varphi}{(J_C + J_V)} \qquad \text{for } \varphi_0 \leq \varphi \leq \varphi_1 \text{ and } \dot{\varphi} < 0 \qquad\qquad (12)$$

$$\dot{\varphi} = -\dot{\theta}$$

5. The drop of the verge in the opposite direction and the acceleration of the crown wheel:

$$\ddot{\theta} = T/J_C \qquad \text{for } \varphi < \varphi_0 \text{ and } \dot{\varphi} \leq 0, \ \int \dot{\theta} dt < \Delta\theta \qquad\qquad (13)$$

$$\ddot{\varphi} = -k\varphi/J_V$$

6. The tooth hits the first pallet.

$$\dot{\varphi}_{after} = \dot{\theta}_{after} = \frac{(\dot{\theta}J_C + \dot{\varphi}J_V)}{J_C + J_V} \qquad\qquad (14)$$
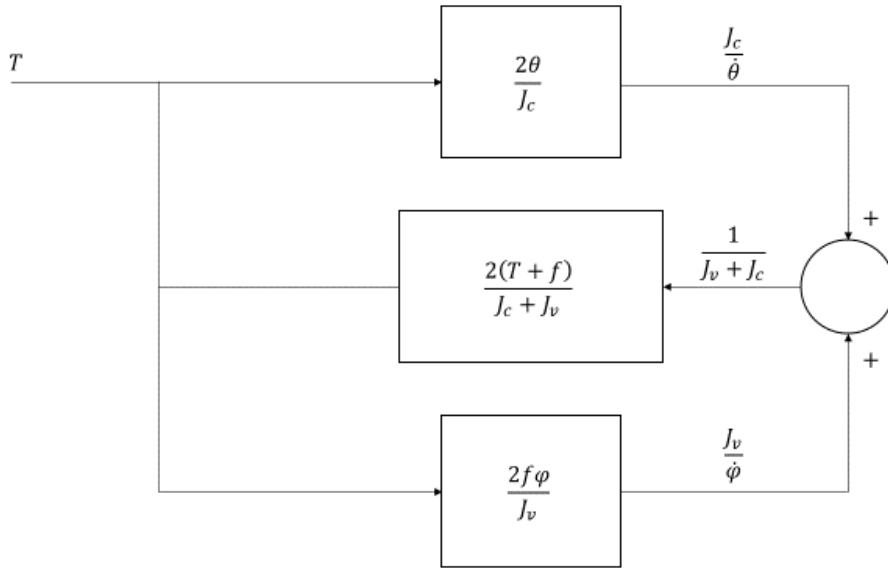
4.4 Stability Analysis

Figure 9 System block diagram of a verge-foliot system

The period of vibration and its relation to friction within the mechanism can be investigated by looking at the piecewise approach used in the previous sections. The first and fourth phases of the mechanism motion are the largest contributors to the period of oscillation. The equations 1 and 4 can be combined as follows:

$$\ddot{\varphi}(J_C + J_V) = -f\,\text{sgn}\dot{\varphi} - T(-1)^n \tag{15}$$

Where f is the frictional torque, T is the torque applied by the hanging drive weight on the mechanism, and n is the number of a pallet in contact with either 1 for the top pallet or two for the bottom pallet.

Building off the work of Andronov et al. (Andronov, Vitt, & Khaikin, 2011), non-dimensional variables can be used as follows:

$$x = \frac{\varphi}{\Delta\varphi}, \quad r = \frac{f}{(J_C + J_V)\Delta\varphi}, \quad \lambda = \frac{T}{(J_C + J_V)\Delta\varphi}, \quad t_{new} = \sqrt{\frac{f}{(J_C + J_V)\Delta\varphi}}\,t \tag{16}$$

This can be applied to Eq. 15, to get

$$\ddot{x} = -r\,\text{sgn}\,\dot{x} - \lambda(-1)^n \qquad (17)$$

The coefficient of friction of the mechanism can be taken to be as follows:

$$\mu = \frac{r}{\lambda} = \frac{f}{T} \qquad (18)$$

The frictional torque f it assumed to be less than the driving torque and given typical values of metal-on-metal friction coefficients, the μ is assumed to be substantially less than 1.

To find the period of oscillation, Eq. 8 is used in conjunction with the non-dimensional variables, yielding

$$\tau_v \approx C\sqrt{\frac{(J_v + J_c)\Delta\varphi}{f}} \qquad (19)$$

The frictional torque can be rewritten, assuming the driving torque, T, is orthogonal to the direction of the frictional force

$$f = \mu T \qquad (20)$$

This follows that Eq. 19 can be rewritten as

$$\tau_v \approx C\sqrt{\frac{(J_v + J_c)\Delta\varphi}{\mu T}} \qquad (21)$$

The stability of the verge-foliot is therefore dependent upon both the friction within the mechanism, and the driving torque of the mechanism itself. However, the driving torque of the mechanism is assumed to be constant, leading to the fact that the change in the coefficient of friction is the largest factor in the stability of the mechanism. If the driving torque is provided by a mainspring, the driving torque will vary over time and cannot be assumed to be constant.

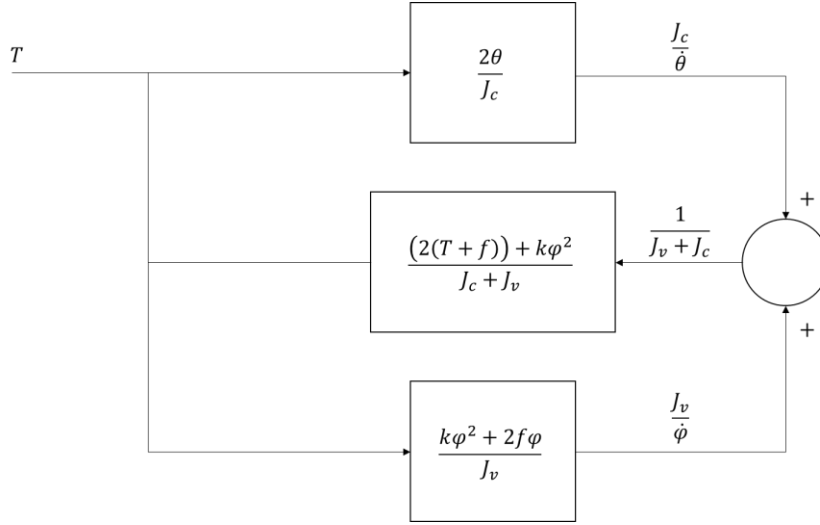## 4.5 Comparison with the Stability of the Pendulum Mechanism

Figure 10 System block diagram of a verge escapement with a pendulum

Extending the approach of the previous section to the pendulum with friction, once again the 1st and 4th phases of vibration are the largest contributors to the oscillation period. As such, Eq. 15 can be modified to include a *k* factor that is the restoring torque.

$$\ddot{\varphi}(J_C + J_V) = -k\varphi - f\,\text{sgn}\dot{\varphi} - T(-1)^n \qquad (22)$$

Applying the non-dimensional variables in Eq. 16, the following dimensionless form is as follows:

$$\ddot{x} = -\Omega^2 x - r\,\text{sgn}\dot{x} - \lambda(-1)^n \qquad (23)$$

The t_{new} can be taken to be $t_{new} = \sqrt{\dfrac{f}{(J_c + J_v)\Delta\varphi}}\, t$ if $k>0$. Assuming $\Omega = 1$ and $r=0$, the period of oscillation is $\tau = 2\pi$. For a $\dfrac{r}{\lambda} \ll 1$, the period is linearly dependent on friction

$$\tau_p\left(\frac{r}{\lambda}\right) \sim 2\pi - C\frac{r}{\lambda} \qquad (24)$$

Converting back to dimensional time units, the period is

$$\tau_p \sim \sqrt{\frac{J_v + J_c}{k}}\,(2\pi - C\mu) \qquad (25)$$

21

Where C is a first order proportionality constant.

To find the stability of both pendulum and the verge mechanisms, a ratio of the variations of the parameter μ with respect to the other variables is used in the following quantities:

$$S_{\mu p} = \frac{1}{\frac{\mu}{\tau}\left|\frac{\partial \tau}{\partial \mu}\right|}, \ S_{\mu v} = \frac{1}{\frac{\mu}{\tau}\left|\frac{\partial \tau}{\partial \mu}\right|} \ (26)$$

These can be approximated to the following:

$$S_{\mu p} \sim 2\pi - \mu, \ \ S_{\mu v} \sim \frac{1}{2\mu} \ (27)$$

The asymptotic nature of the stability of the verge with relation to the coefficient of friction, $S_{\mu v}$, coupled with keeping the coefficient of friction substantially less than 1, $\mu \ll 1$, any variation in the coefficient of friction results in a substantial change in the period of oscillation.

The linear nature of the stability of the pendulum with relation to the coefficient of friction, $S_{\mu p}$, coupled with keep the coefficient of friction substantially less than 1, $\mu \ll 1$, any variation in the coefficient of friction results in a relatively insignificant change in the period of oscillation.

The relation between $S_{\mu p}$ and $S_{\mu v}$ can be further illustrated by taking the ratio of the equations 27, resulting in

$$\frac{S_{\mu p}}{S_{\mu v}} = \frac{\pi}{\mu} - \frac{1}{2} \ \ \ (28)$$

Using a coefficient of friction of $\mu = 0.1$, which is a typical approximation for a lubricated, metal on metal mechanism (Blumenthal & Nosonovsky, 2020), Eq. 28 becomes

$$\frac{S_{\mu p}}{S_{\mu v}} \approx 31 \ \ \ (29)$$

The value of Eq. 24 is in line with statements of the increase of accuracy of the pendulum clock over the verge-foliot mechanism. Furthermore, referring to equations 21 and 25 to solve the periods of the oscillation of the verge with and without a pendulum, the $\tau_v \propto \Delta\varphi$ while τ_p does not include a term relating to the amplitude of the oscillation; this relates to the property of isochronicity, where the frequency of the oscillation is independent of the amplitude of the oscillation. Therefore, within small vibrations, the amplitude of the oscillation of a pendulum can be approximated as having no impact on the period of the motion. Tautochrone curves, first discussed by Christian Huygens, are cycloid curves that take the same time to travel down without friction under the force of gravity no matter how far up the curve they are brought.

5. Experimental Modeling of The Verge-And-Foliot Mechanisms

In this section, I developed an FEA experiment to test the previously developed mathematical model of the verge-foliot and pendulum-verge mechanisms. CAD models of both mechanisms are developed using historical examples as guides. These models are then used in an FEA software package to iteratively simulate a variety of conditions that would be prohibitively difficult to experiment on physical models.

5.1 Methods Used

To test the validity of the mathematical model, I developed an empirical model of the clock. I pursued several methods before arriving on the use of FEA simulations.

Initially, I had planned on making a physical model of a clock and taking measurements off the movement of the clock using a Hall-effect sensor to measure the oscillation of foliot weights made of magnets. I planned on using the serial function of an Arduino to print out the data and post-processing this using MATLAB code.

Without access to the necessary tools and expertise to build a clock using traditional materials and methods, I instead decided to develop a clock to be printed out using PLA, using a Prusa I3 MK3S 3D

printer. The 3D printer I used utilizes the FDM/FFF process, where a nozzle moves in a 2-D plane depositing material before being lifted a maximum distance less than the thickness of the consumable material to begin again, and usually within the range of 0.05 mm to 0.3 mm. The consumable material, called filament, is usually a thermoplastic in the form of a long, continuous strand of 3 mm diameter or less, with 1.75 mm diameter strands being the most commonly available. This filament is fed through a nozzle heated above the melting point of the filament material, then deposits the filament onto a heated bed. Due to this layering occurring in visibly large increments, the surface texture can be rough and have a high friction coefficient, while the bulk solid material exhibits anisotropic properties. With proper selection of the printing orientation, the anisotropy can be used to benefit the strength of the printed model. The tradeoff for changing the orientation of a print is that more support material to build the model on is necessary.

To develop G-code to send to the printer, I developed a clock in CAD based off a variety of images of clocks available, an understanding of the going train of a verge-foliot clock, and prior work with involute gear trains. A thorough understanding of the operation of the verge-foliot was based off the descriptions by F.J Britten in his treatise *Britten's Old Clocks and Watches and Their Makers*. An article in the August 1964 edition of the magazine *Popular Mechanics* is titled "Early Swiss Wooden-Wheel Clock" by E.R. Haan and provides plans to build a wooden verge-foliot clock; however, despite the assertion that the clock is in a Medieval style, no supporting explanation is given as to where these plans are derived from.

To get the teeth to mesh using standard ISO spur gears, a module of 1 was used and the tooth counts were changed to the following: main wheel has 80, second has 48, hour has 48 and crown wheel has 21 teeth. The pinions chosen to have 8 trundles on the second pinion, 8 trundles on the escape pinion, and 4 trundles on the hour pinion; these were chosen to better mesh with the available ISO spur gears. The *field gate* style frame of the original was used in construction of the model clock to support the wheels and components.

The manner of assembly and production of parts was taken into consideration as well. A crown wheel consisting of trundles or outward facing wire spokes was used, along with pinion gears. The simple shape and manner of assembly was chosen to be easier to print or use wire if necessary. Collets and arbors provide a method of properly positioning gears and pinions. Locational transition fits (H7/n6 hole basis, N7/h6 shaft basis) when possible are used to hold parts in place and close running fits (H8/f7 hole basis, F8/h7 shaft basis) are used for parts that are required to rotate (Oberg, et al., 2020).

The software used to build the clock was Dassault Systèmes SolidWorks 2018 Version 26 (Dassault Systèmes, 2018). The software provides parametric modeling that allows for multiple parameters to be changed simultaneously and automatically, making it easy to change size of the clock or other relations within the clock CAD file. The SolidWorks Toolbox, Motion and Simulation add-in toolboxes were activated and used throughout the modeling of the clock. The Toolbox add-in was especially helpful for its library of readily modifiable gears and components. The ISO library of Power Transmission parts was used to create ISO spur gears. The Simulation add-in has material choices that can be made for any parts in the assembly, and this functionality was used to improve the accuracy of dynamic modeling and to give more realistic results for analysis and comparison with known clocks that had both the verge-foliot and pendulum-anchor escapements. This quick check in the native SolidWorks environment meant I could avoid iterating needlessly.

After printing the clock from the CAD model, as shown in Fig. 11, and assembling it, I began to troubleshoot its operation. Despite taking care in the orientation of parts on the print bed, due to the limitations in the size of the print bed, the sheer force of the impact on the pallets of the verge would break. However, when I reinforced the pallets, the impact then would break off pegs on the escape wheel. The surface finish of the parts introduced unaccounted for friction in the going train that then required a heavier driving weight to get the clock in motion, and I had trouble controlling the friction between not

only the pallets and escape wheel, but all the bushings as well. As a result of the difficulties in getting the clock to work, I switched to developing the experimental set-up in an FEA simulation environment instead.
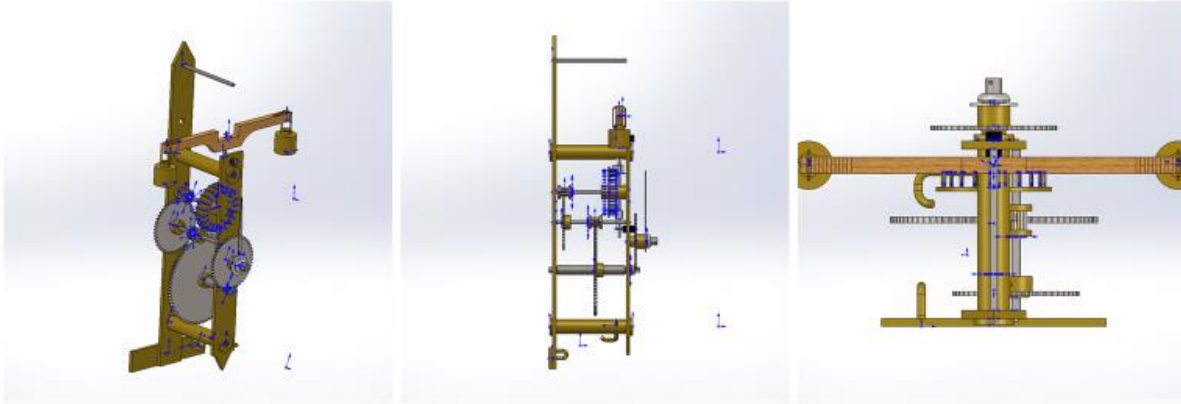

Figure 11 CAD of clock using a proven going train

5.2 Set-Up of Experiment

The CAD models of both the verge-foliot and pendulum-verge mechanisms, were put into the ANSYS R2 FEA software environment (Ansys Inc., 2020). To test the kinematic model, the Explicit Dynamic system environment was chosen; this environment is best suited for non-linear problems with impacts. To reduce the computational cost of the simulation, I stripped the mechanism down to just the verge, the pendulum or foliot with weights, and the escape wheel. I used revolute body-ground joints on both verge and escape wheel and created a frictional body interaction connection constraint. Both bodies were set to rigid body stiffness behavior and assigned the C37700 brass material. A moment applied to escape wheel of 226047 $N \cdot mm$ was the driving condition, and solutions of displacement, velocity and acceleration were chosen. With coarse mesh resolution, it still took the computer with a network of three computers to run the simulation around 14 minutes to complete each experiment. I set the experiment to produce an output of 15 seconds, after several simulations showed that a break-in period occurs before the mechanism settles into its more stable oscillation. I tried both a Modal and a Harmonic Response environment on the

verge-foliot, however, as predicted mathematically, the computer failed to produce a natural frequency after a run time of around 5 hours.

5.3 Results

Using the FEA software and models of both verge-foliot and pendulum-verge mechanisms, numerical outputs of various parameters were produced in relation to time. The charts in Fig. 13 to 18 were created using these output data from a probe on a node with a known radius from the axis of rotation. Fig. 13 shows the angular displacement in radians of the verge-foliot mechanism. After a break-in period of around three seconds, the oscillation stabilizes.   Fig. 14 shows the angular velocity of the verge-foliot mechanism from the same node. Fig. 15 shows the angular acceleration of the verge-foliot. Fig. 16 shows the angular displacement in radians of the pendulum-verge mechanism. After a break-in period of around two and a quarter seconds, the oscillation stabilizes.   Fig. 17 shows the angular velocity of the pendulum-verge mechanism from the same node. Fig. 18 shows the angular acceleration of the pendulum-verge.
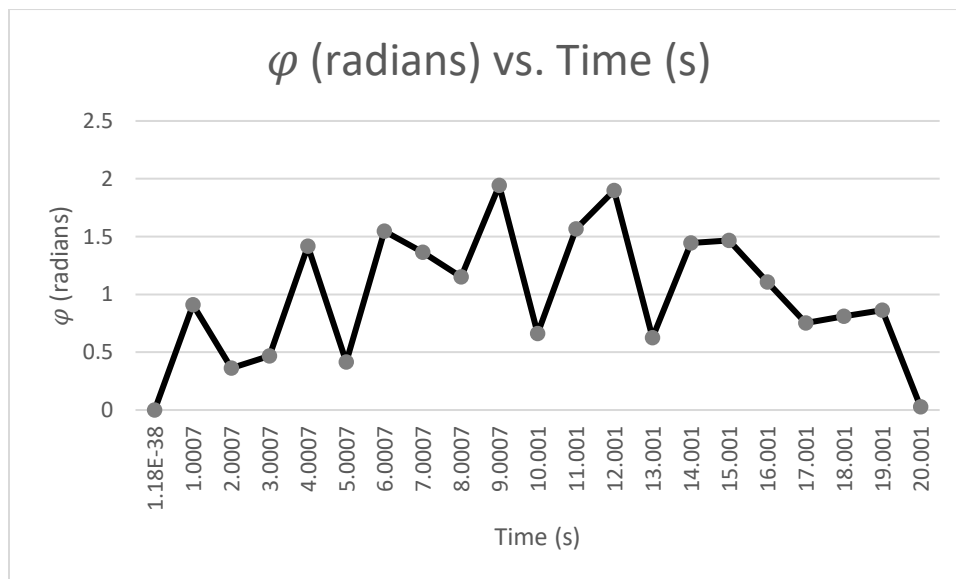

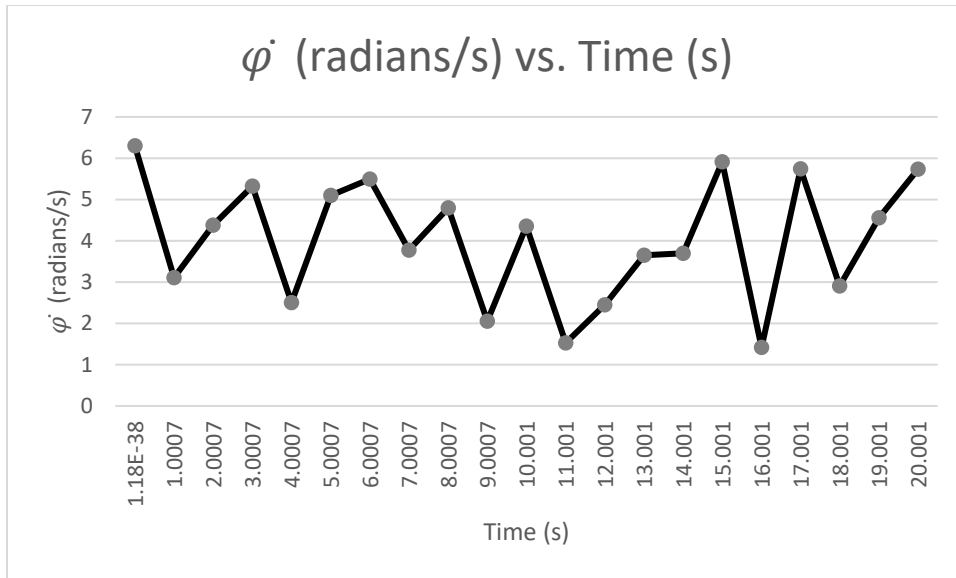**Figure 12 Angular Displacement of the Verge-Foliot**

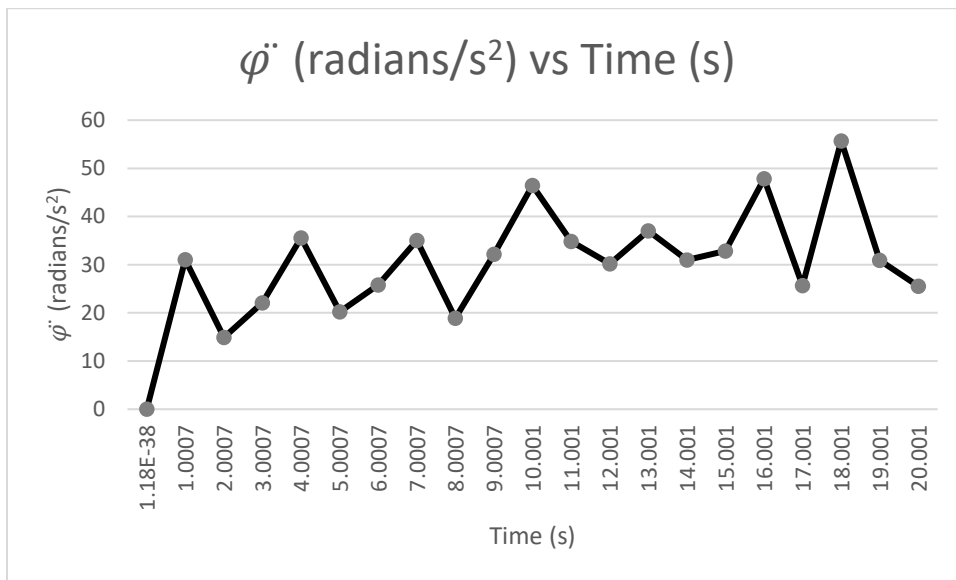**Figure 13 Angular Velocity of the Verge-Foliot**

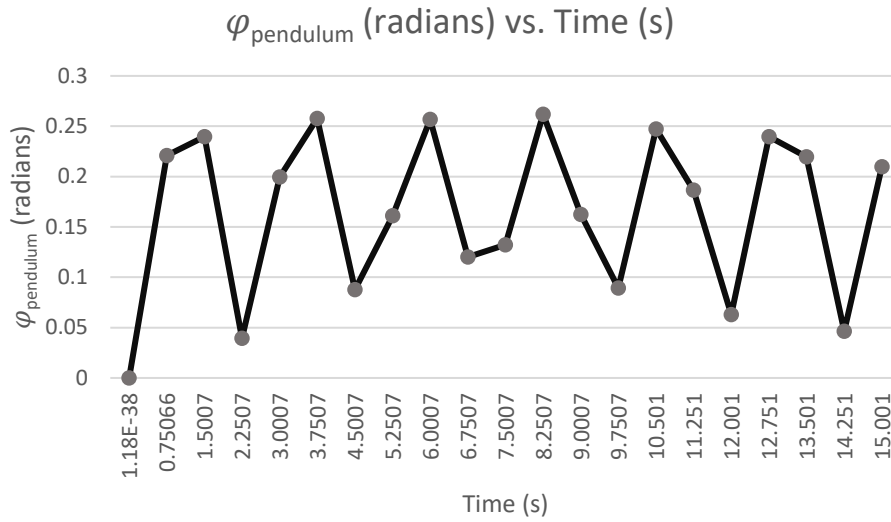**Figure 14 Angular Acceleration of the Verge-Foliot**

Figure 15 Angular Displacement of the Pendulum-Verge

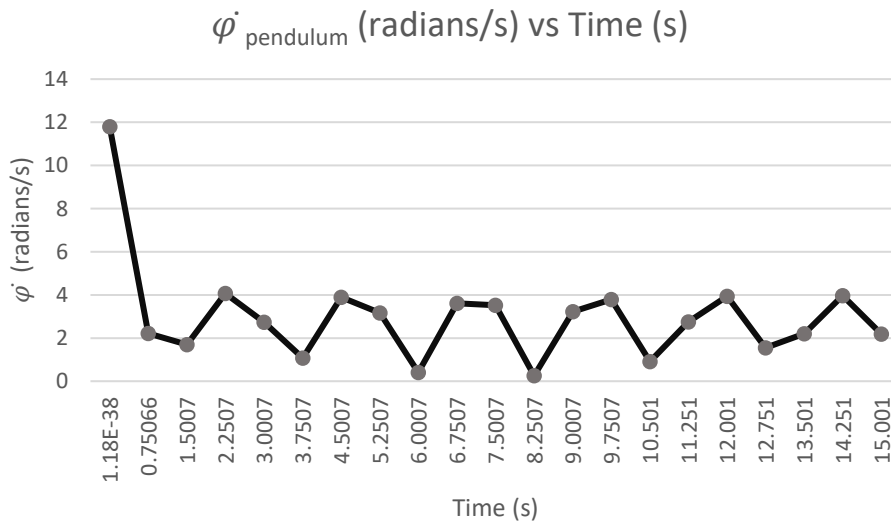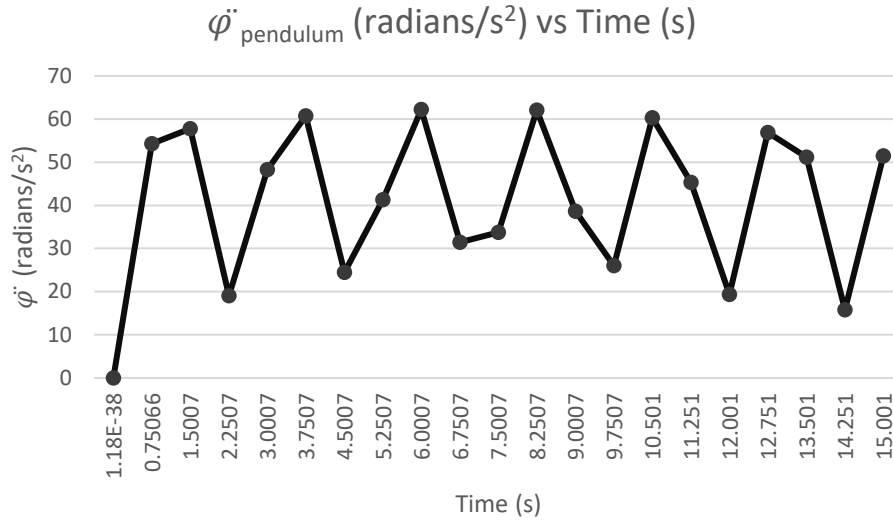**Figure 16 Angular Velocity of the Pendulum-Verge**

Figure 17 Angular Acceleration of the Pendulum-Verge
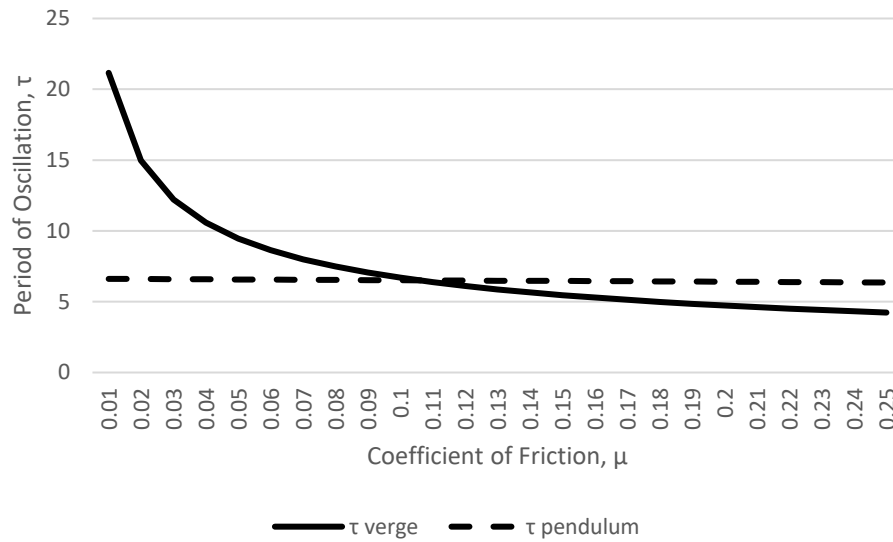

Figure 18 Dependency of Period of Oscillation on the Coefficient of Friction

5.4 Discussion

The FEA experiment confirmed the mathematical model to approximate the empirical findings. The period

of oscillation experimentally for the pendulum is 4.494 seconds, while the experimentally tested period

for the verge-foliot is 6.003 seconds. Assuming C=1, the periods of oscillation are 6.692 seconds for the

verge and 6.516 seconds for the pendulum. The experimental error of the verge-foliot was 10.3%, while

the experimental error for the pendulum-verge is 31%. The experimental error of both mechanisms can

be explained by simplifications in both the mathematical model and the FEA solver. In the mathematical

model, we assumed that all the collisions are inelastic, and we accounted for a variety of factors using the

scaling constant C. In the FEA experiment, I kept the bodies rigid, but by doing so, the collisions are

approximated as elastic collisions, with little dissipative energy loss. The effects of this retention of the

energy in collisions is best seen in Fig. 15, where there is a slight upward trend in the acceleration of the

foliot, indicating that the mechanism is decreasing its period over time and therefore moving away from

being a stable harmonic oscillator. The FEA solver also reduced the number of output points to decrease

the computational expense of running a complex non-linear problem but reduces the accuracy of the

measurement and increases the risk of aliasing data. I also only included friction in the contact between

the escape wheel and the verge pallets, however, the frictional losses in the mathematical model also

extend into the bushings of the mechanisms. This was hard to account for in the FEA model, because I

reduced the number of components to limit the number of solver output cycle iterations required, thereby

reducing the runtime of the experiment.

The verge-foliot had variance in its motion, as seen in Fig. 13, 14 and 15. In Fig. 13, the angular

displacement of the verge-foliot, while clearly oscillatory, still has a fair amount of noise. I struggled to get

a good balance between the number of output points for appropriate fidelity. When I programmed the

simulation to produce 500 output points, the simulation ran for 101 minutes, and showed a high degree

of aliasing. Due to the lack of a natural frequency of the verge-foliot system, it is hard to establish proper

sampling rates. Fig. 14 also, shows this trend of deviation, however, this deviation from the midline

coincides with the instability of the verge shown in the mathematical model. The assumption that the

normal force component of the frictional force is not necessarily always true in the CAD model, and

therefore the frictional force could be less than what the mathematical model is expecting. This deviation could be a result of a variety of factors ranging from the angle of the pallet in relation to the rounded tip of the escape wheel pegs to the size of the mesh applied and the nodes not contacting in a consistent manner. As previously mentioned, the acceleration of the verge in Fig. 15 has a slight upward trend due to the smaller reduction in energy in the system than would otherwise be expected.

The oscillation of the verge-foliot mechanism in Fig. 12, 13 and 14 could also be explained by some amount of noise corruption occurring. Oscillating functions, as alluded to before, could be viewed as a combination of sinusoidal waves, and as a result aliasing needs to be considered. I increased the sampling frequency from $f_s = 1.33$ Hz to $f_s = 6.66$ Hz, however, the noise was still there. I applied a Fourier Transform to the data to move it into the frequency domain and be able to better look at the dominant frequencies in the oscillation. The dominant frequency appeared to be on the y-axis, roughly 0 Hz. Applying a high-pass filter at 0.063 Hz, the dominant frequency became $f_{dominant} = 0.1201$ Hz, corresponding to a $\tau_{dominant} = 8.324$ seconds. The period of the dominant frequency corresponds to an experimental percent error of 24.4%, which is a little more than double the experimental of the period determined by observing the clock and going frame-by-frame at 10.3%. The combination of other

The pendulum-verge, as illustrated in Fig. 16, 17 and 18, has an approximate harmonic oscillation. As stated in the mathematical model, the restoring torque of the pendulum and the natural frequency of the pendulum stabilize the system to outside factors. Fig. 17, the angular velocity of the pendulum, illustrates the break-in period necessary for any mechanism to stabilize after the breaking force required to overcome static frictional forces.

6. Conclusions

In this thesis a mathematical model was developed to investigate the reason verge-foliot mechanisms were substantially less accurate than pendulums with a verge mechanism. The effect of friction on the

stability of both the verge-foliot and the pendulum mechanisms was investigated and obtained insights

on the improved performance of the pendulum using computer simulations of both mechanisms. The

verge-foliot was shown to be a non-linear system both mathematically and empirically. The output of the

FEA analysis of the verge-foliot indicated a system with a high degree of noise that was explained due to

a combination of the nodal mesh size at contacts, rigid body assumptions and elastic collisions. The

relative lack of noise in the signal of the pendulum-verge along with the mathematical model indicates a

system with a high degree of stability, a natural frequency and is comparatively linear.

The verge-foliot was very sensitive to variation in the friction coefficient, μ. The stability of the verge-foliot

had an inverse relationship with friction, as opposed to the stability of the pendulum having a linear

friction relationship. The decrease in sensitivity due to the restoring torque of the pendulum provided a

clock with an increase in both precision and accuracy. When calculated, this increase in accuracy was

shown to be roughly 31 times at a friction of $\mu = 0.1$. This improvement led to the isochronicity of

pendulums and other modern clock movements.

The history of tower clocks starting in the 13th century CE, and the change brought about by the invention

of the pendulum by Christiaan Huygens was discussed. The implications of this rapid improvement in clock

mechanisms were shown to be not only in the accuracy of the mechanism, but also in the proliferation of

clocks and in the construction of these clocks as well. Improvements in the accuracy of timekeeping pieces

impacted the advancement of society in general and was shown to spur the development of a variety of

sciences.

The development of clock models in CAD and FEA simulation simulations was discussed. A discussion of

the pitfalls of 3D printing manufacturing processes was also discussed. The limitations of FEA analyses

were also shown.

REFERENCES

al-Razzaz al-Jazari , B.-Z. i., & `Abd al-Latif, F. i. (1315). "The Elephant Clock", Folio from a Book of the Knowledge of Ingenious Mechanical Devices by al-Jazari. *Book of the Knowledge of Ingenious Mechanical Devices.* Metropolitan Museum of Art, New York City. doi:57.51.23

Andronov, A. A., Vitt, A. A., & Khaikin, S. E. (2011). *Theory of Oscillators* (Vol. 4). (W. Fishwick, Ed., & F. Immirzi, Trans.) Mineola, NY, USA: Dover Publications, Inc.

Ansys Inc. (2020). ANSYS Mechanical. *R2*. Canonsburg, PA, USA: Ansys Inc.

Bisgaard, M. (2006, August 7). *File:Tidens naturlære fig21.png.* Retrieved from Wikimedia Commons: https://commons.wikimedia.org/w/index.php?title=File:Tidens_naturl%C3%A6re_fig21.png&old id=474568737

Blumenthal, A. S., & Nosonovsky, M. (2020). Friction and Dynamics of Verge and Foliot: How the Invention of the Pendulum Made Clocks Much More Accurate. *Applied Mchanics*, 11-122. doi:10.3390/applmech1020008

Brearley, H. C. (1919). *Time Telling Through the Ages.* New York City: Doubleday, Page for Robert H. Ingersoll & Bro., New York.

Britten, F. J., Clutton, C., Baille, G. H., Baillie, G. H., & Ilbert, A. C. (1973). *Britten's Old Clocks and Watches and Their Makers.* New York City: Bonanza Books.

Bruton, E. (2004). *The History of Clocks & Watches.* Edison, NJ, USA: Chartwell Books.

Cipolla, C. M. (2003). *Clocks and Culture 1300-1700.* New York City: W. W. Norton & Company.

Conover, S. G. (2000). *How to Make a Foliot Clock.* Reading, PA, USA: Clockmakers Newsletter.

Dassault Systèmes. (2018). SolidWorks Version 26 . *SolidWorks*. Boston, MA, USA: Dassault Systèmes.

de Dondi, G. (1461). *File:Giovanni Di Dondi clock.png.* Retrieved from Wikimedia Commons: https://commons.wikimedia.org/wiki/File:Giovanni_Di_Dondi_clock.png

Denning, C. (2007, October 14). *File:Cotehele Clock 01.jpg.* Retrieved from Wikimedia Commons: https://commons.wikimedia.org/w/index.php?title=File:Cotehele_Clock_01.jpg&oldid=4909900 99

Evans, G. R. (2007). The Meaning of Monastic Culture: Anselm and His Contemporaries. In J. G. Clark (Ed.), *The Culture of Medieval English Monasticism* (pp. 75-85). Woodbridge, Suffolk, UK: Boydell & Brewer.

Frank, M. (2008, May). *Wagner Remontoir*. Retrieved from MY-TIME-MACHINES: http://www.my-time-machines.net/wagner_remontoir.htm

Frank, M. (2013). *The Evolution of Tower Clock Movements and Their Design Over the Past 1000 Yearks*. Retrieved from MY-TIME-MACHINES: http://www.my-time-machines.net/speech_final_web.pdf

Glasgow, D. (1885). *Watch and Clock Making.* London: Cassell & Company, Limited.

Haan, E. R. (1964, August). Early Swiss Wodden-Wheel Clock. *Popular Mechanics*, pp. 156-159.

Headrick, M. V. (2002). Origin and evolution of the anchor clock escapement. *IEEE Control Systems Magazine*, 41-52. doi:10.1109/37.993314

Honnecourt, V. (1230). *Villard de Honnecourt - Sketchbook - 44.jpg.* Retrieved from Wikimedia Commons: https://commons.wikimedia.org/w/index.php?title=File:Villard_de_Honnecourt_-_Sketchbook_-_44.jpg&oldid=201780768

Houtkooper, W. (1992). The Accuracy of the Foliot. (E. J. Tyler, Ed.) *Antiquarian Horology*, 74-75.

IEEE Tokyo Section. (2004, November 25). *Milestones:Electronic Quartz Wristwatch, 1969*. Retrieved from ETHW: https://ethw.org/Milestones:Electronic_Quartz_Wristwatch,_1969

Kleinschmidt, H. (2000). Generalities. In H. Kleinschmidt, *Understanding the Middle Ages: The Transformation of Ideas and Attitudes in the Medieval World* (pp. 24-30). Woodbridge: Boydell & Brewer.

Lepschy, A. M., Mian, G. A., & Viaro, U. (1992). Feedback Control in Ancient Water and Mechanical Clocks. *IEEE Transactions on Education*, 3-10. doi:10.1109/13.123411

Lienhard, J. H. (2000). *NO. 1506: THE FIRST MECHANIAL CLOCKS*. Retrieved from Engines of Our Ingenuity: https://uh.edu/engines/epi1506.htm

Llewelyn, H. (2014, July 28). *File:Salisbury Cathedral (St. Mary).* Retrieved from Wikimedia Commons: https://commons.wikimedia.org/w/index.php?title=File:Salisbury_Cathedral_(St._Mary)_(14850828041).jpg&oldid=463455210

Lombardi, M. (2007, March 5). *Why is a minute divided into 60 seconds, an hour into 60 minutes, yet there are only 24 hours in a day?* Retrieved from Scientific American: https://www.scientificamerican.com/article/experts-time-division-days-hours-minutes/#:~:text=Hipparchus%2C%20whose%20work%20primarily%20took,darkness%20observed%20on%20equinox%20days.

Marrison, W. A. (1948). The Evolution of the Quartz Crystal Clock. *The Bell System Technical Journal*, 510-588.

McKay, C. G. (2016). Winding. In C. G. McKay, *The Turret Clock Keeper's Handbook* (pp. 19-21). Dorset: The AHS Turret Clock Group.

Moon, F. C., & Stiefel, P. D. (2006). Coexisting Chaotic and Periodic Dynamics in Clock Escapements. *Philosophical Transactions: Mathematical, Physical and Engineering Sciences*, 2539-2563.

Mumford, L. (2010). The Monastery and the Clock. In L. Mumford, *Technics & Civilization* (pp. 12-18). Chicago: The University of Chicago Press.

Oberg, E., Jones, F. D., Horton, H. L., Ryffel, H. H., McCauley, C. J., & Brengelman, L. (2020). Gears and Gearing. In E. Oberg, F. D. Jones, H. L. Horton, H. H. Ryffel, C. J. McCauley, & L. Brengelman, *Machinery's Handbook 31st Edition* (pp. 2204-2255). South Norwalk: Industrial Press, Inc.

Peel, M. (2012, December 21). *File:Salisbury Cathedral 2012 12.jpg.* Retrieved from Wikimedia Commons: https://commons.wikimedia.org/w/index.php?title=File:Salisbury_Cathedral_2012_12.jpg&oldid=442186977

Price, D. J. (1959). On the Origin of Clockwork, Perpetual Motion Devices, and the Compass. *Contributions from the Museum of History and Technology*, 81-112.

Randall, A. G. (1978). Constant Force Escapements and an Escapement Remontoire. *Antiquarian Horology*, 46-60.

Robertson, J. J., & O'Connor, E. F. (1999). *Hipparchus of Rhodes*. Retrieved from MacTutor: https://mathshistory.st-andrews.ac.uk/Biographies/Hipparchus/

Robertson, J. J., & O'Connor, E. F. (2010, May). *Jost Bürgi.* Retrieved from MacTutor: https://mathshistory.st-andrews.ac.uk/Biographies/Burgi/

Speiser, D. (2008). Huygens's Horologium Oscillatorium and Newton's Principia. In D. Speiser, K. Williams, & S. Caparrini (Eds.), *Discovering the Principles of Mechanics 1600-1800* (pp. 41-45). Therwil: Birkhäuser.

Usher, A. P. (2011). Water Clocks and Mechanical Clocks: 16 B.C-A.D 1500. In A. P. Usher, *History of Mechanical Inventions* (pp. 187-198). New York City: Dover Publications.

Vaughn, T. (2019). *https://www.newenglandhistoricalsociety.com/eli-terry-connecticut-clock-maker/*. Retrieved from New England Historical Societyt: https://www.newenglandhistoricalsociety.com/eli-terry-connecticut-clock-maker/

Wilcox, M. (2014, March 18). *COLUMBUS CLOCK*. Retrieved from Value This Now: http://blog.valuethisnow.com/posts/columbus-clock

Zheleztsov, N. A. (2011). 5. Theory of the Clock, Model of a "Recoil Escapement" without Impulses". In A. A. Andronov, S. E. Khaikin, A. A. Vitt, & W. Fishwick (Ed.), *Theory of Oscillators* (I. F., Trans., Vol. 4, pp. 183-199). Mineola, NY: Dover Publications, Inc.

APPENDIX

Appendix A

I broke the model down into a piecewise function of six parts that describe the above action. First, using

the Lagrange Formulism, I figured out the work-energy of each component in each of the six above states.

Second, the Formulism is used. Third, moments of inertias are substituted in. This process results in the

following set of equations, each lasting for $\frac{\kappa\pi}{n3}$, where k is equal to any positive, non-zero cardinal number.

1. Clockwise Impulse

$$\left(m_{cr} \cdot R_{cr}^2 + 2 \cdot \frac{R_{cr}^2}{R_{vf}^2} \cdot M \cdot l^2 + m_{drive} \cdot R_{drive}^2 \right) \cdot \ddot{\varphi} - m_{drive} \cdot g \cdot R_{drive} = 0$$

2. Clockwise Free Rotation

$$\left(m_{cr} \cdot R_{cr}^2 + m_{drive} \cdot R_{drive}^2 \right) \cdot \ddot{\varphi} - m_{drive} \cdot g \cdot R_{drive} = 0$$

$$\left(2 \cdot \frac{R_{cr}^2}{R_{vf}^2} \cdot M \cdot l^2 \right) \cdot \ddot{\omega} = 0$$

3. Counterclockwise Contact

$$\left(m_{cr} \cdot R_{cr}^2 + m_{drive} \cdot R_{drive}^2 \right) \cdot \ddot{\varphi} - 2 \cdot \frac{R_{cr}^2}{R_{vf}^2} \cdot M \cdot l^2 \cdot \ddot{\omega} - m_{drive} \cdot g \cdot R_{drive} = 0$$

38

4. Counterclockwise Impulse

$$\left(m_{cr} \cdot R_{cr}^2 + 2 \cdot \frac{R_{cr}^2}{R_{vf}^2} \cdot M \cdot l^2 + m_{drive} \cdot R_{drive}^2 \right) \cdot \ddot{\varphi} - m_{drive} \cdot g \cdot R_{drive} = 0$$

5. Counterclockwise Free Rotation

$$(m_{cr} \cdot R_{cr}^2 + m_{drive} \cdot R_{drive}^2) \cdot \ddot{\varphi} - m_{drive} \cdot g \cdot R_{drive} = 0$$

$$\left(2 \cdot \frac{R_{cr}^2}{R_{vf}^2} \cdot M \cdot l^2 \right) \cdot \ddot{\omega} = 0$$

6. Clockwise Contact

$$(m_{cr} \cdot R_{cr}^2 + m_{drive} \cdot R_{drive}^2) \cdot \ddot{\varphi} - 2 \cdot \frac{R_{cr}^2}{R_{vf}^2} \cdot M \cdot l^2 \cdot \ddot{\omega} - m_{drive} \cdot g \cdot R_{drive} = 0$$

While at first glance these equations seem to contradict the motion of the verge-foliot, it is important to remember that the two opposing paddles on the verge ensure that the application of forces relative to the crown gear's rotation remain in the same direction, however, with two different outcome directions for the verge-foliot.
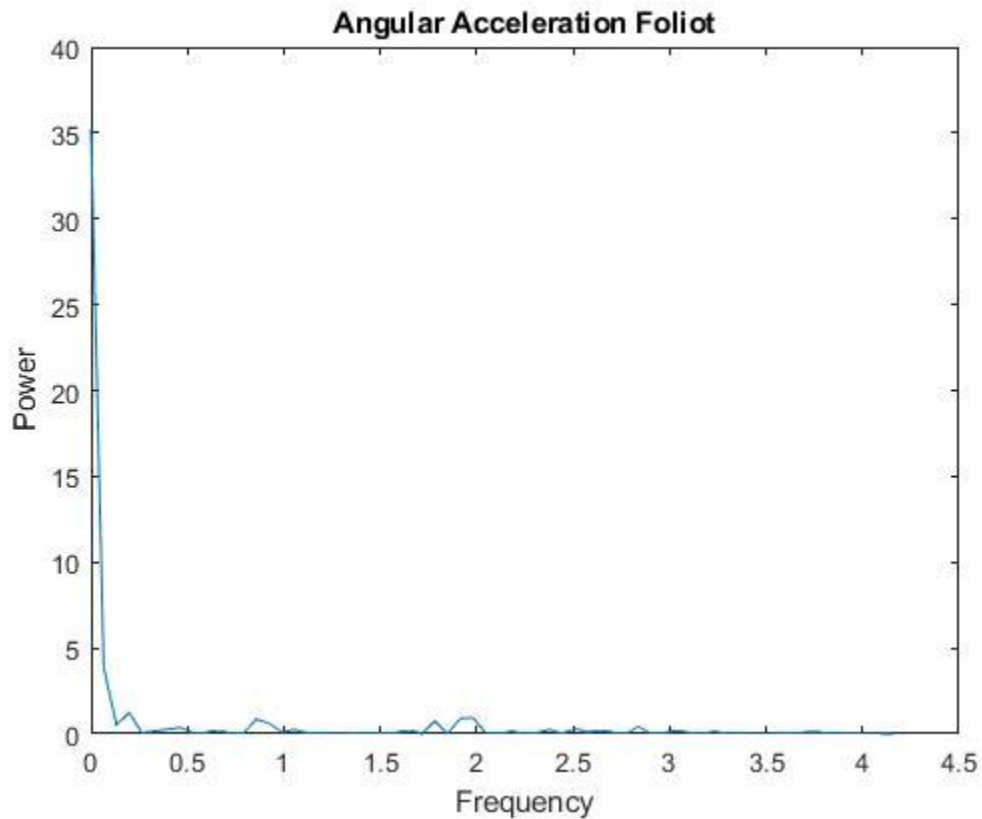
Figure 19 Fourier Transform of Angular Displacement

```
clc; clf; clear;

opts = detectImportOptions('500pointsdata.xlsx');
preview('500pointsdata.xlsx',opts)
opts.Sheet = 'Explicit_Dynamics_dis100nprobe';
opts.SelectedVariableNames = [2,4];
opts.DataRange = '2:102';
M = readmatrix('500pointsdata.xlsx',opts);
t = M(:,1);
x = M(:,2);
figure(11)
plot(t,x);
y = fft(x);
f = (0:length(y)-1)*(100/15)/length(y);
figure(12)
plot(f,abs(y))
title('Magnitude')
n = length(x);
fshift = (-n/2:n/2-1)*(1/n);
yshift = fftshift(y);
figure(13)
plot(fshift,abs(yshift))
rng('default')
```

```matlab
xnoise = x;
ynoise = fft(xnoise);
ynoiseshift = fftshift(ynoise);
power = abs(ynoiseshift).^2/n;
figure(14)
plot(fshift,power)
title('Power')
m = length(x);
n = pow2(nextpow2(m));
y = fft(x,n);
power = abs(y).^2/n;    % power spectrum
figure(15)
plot(f(1:floor(n/2)),power(1:floor(n/2)))
title('Angular Acceleration Foliot')
xlabel('Frequency')
ylabel('Power')
figure(1)
highpass(f(1:floor(n/2)),0.063,(100/15))
[yfilter,d]=highpass(f(1:floor(n/2)),0.063,(100/15));
ymax=max(yfilter);
```
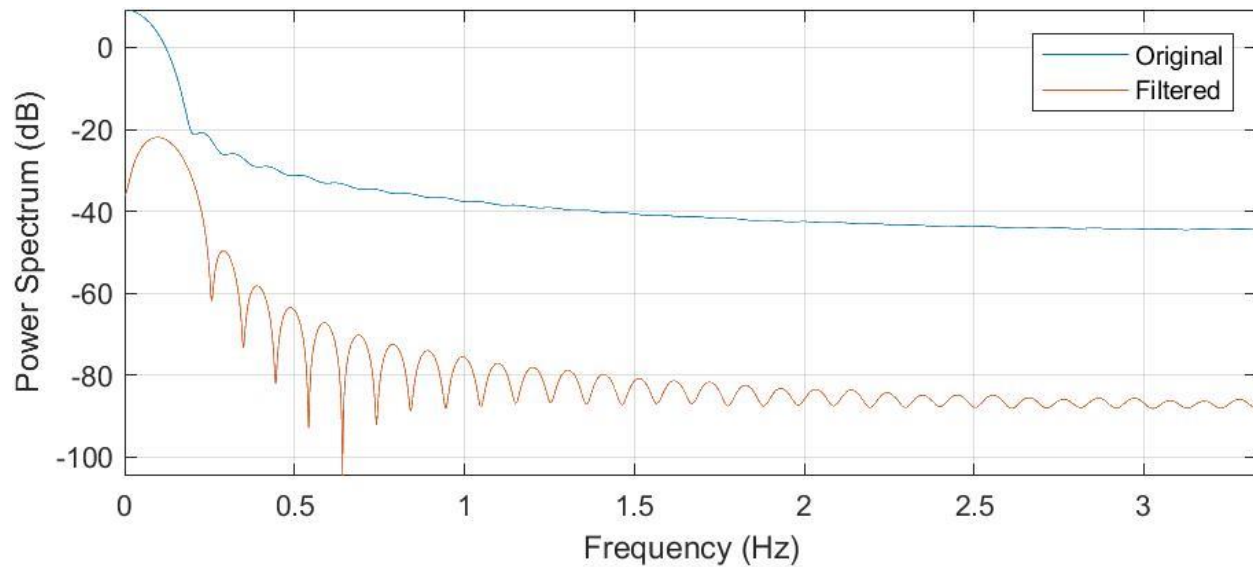

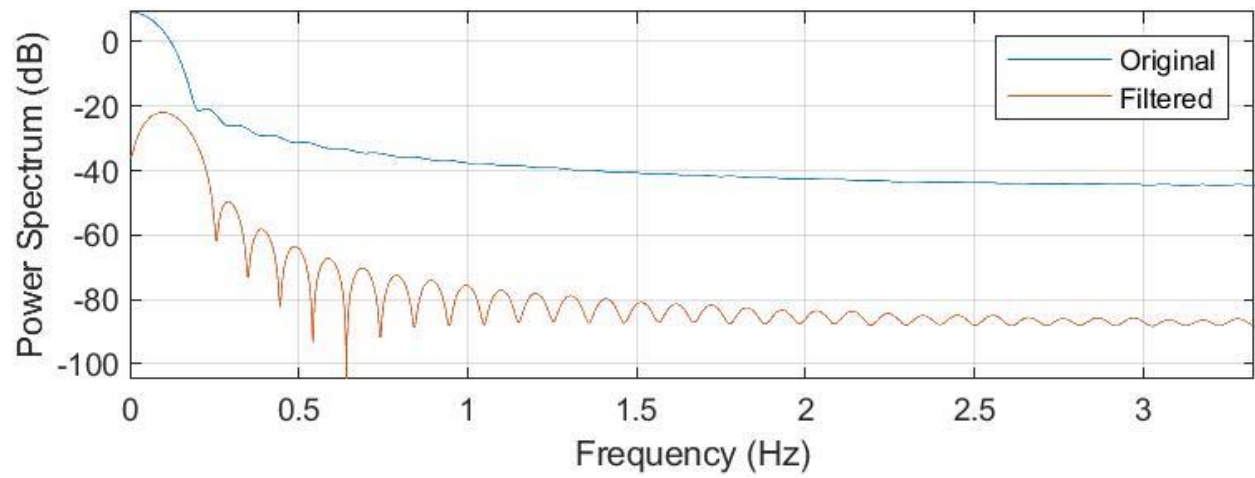**Figure 20 High Pass Filter at 63 mHz Application of Verge-Foliot Acceleration**

Figure 21 High Pass Filter at 63 mHz Application of Verge-Foliot Displacement in the Frequency Domain